Computational haemodynamics in stenotic internal jugular veins

Gino I. Montecinos[1]*, Alfonso Caiazzo[1], Lucas O. Müller[1], Eleuterio F. Toro[1] and E.M. Haacke[2]

[1]University of Trento, Italy [2]Wayne State University, Detroit, USA

Introduction

Stenoses are normally defined according to generic anatomic criteria, as the reduction of internal jugular vein (IJV) cross-sectional area (CSA) below a fixed threshold[7;8]. However, the entity of the occlusion might have different impact on the hemodynamics, according to patient specific features, as the venous anatomy and the existence of collateral paths. The goal of this work is to provide a computational framework to assess the relevance of IJV stenoses based on mechanical considerations and taking into account a patient-specific context.

First, a numerical simulation of blood flow is carried out on a three-dimensional mesh obtained from MRI images segmentation, using patient specific cerebral blood flow data. Starting from the original healthy configuration, artificial stenoses of different entities are introduced, via a local deformation of the segmented surface. To take into account the existence of collateral paths, different simplified networks of the major cerebral veins have been included in the computational study via a multiscale 3D-1D model.

Computational Fluid Dynamics (CFD) is then applied on different multiscale configurations, in order to quantify the effect of the stenosis on the cerebral hemodynamics on a global level. In particular, we monitor the magnitude of pressure drop along the stenotic IJVs and the behavior of wall shear stress (WSS), which might be responsible for vascular damages[2;5].

Methodology

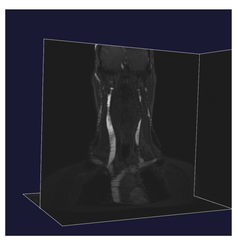

A snapshot of the image segmentation procedure (using VMTK). MRI data courtesy of Dr. E.M. Haacke.

Image segmentation. Three-dimensional patient geometries have been obtained from MRI data segmentation. From the original images (DICOM sequence) , we segmented the two IJVs and brachiocephalic veins, up to the superior vena cava and the subclavian veins.

Segmentation has been performed using the open-source software VMTK (*Vascular Modeling ToolKit*,[1]), which provides triangulated surface representations. The computational volume meshes have been created using the open-source mesh generator TetGen[3].

Reduction of CSA. Starting from the segmented geometry (healthy configuration), artifical reduction of CSA has been achieved via a local deformation of the computational domain. This deformation has been obtained solving a partial differential equation describing the behavior of an elastic material:

$$\begin{cases} \nabla \cdot \sigma(\mathbf{d}) = 0, & \text{on } \Omega \\ \mathbf{d} = \mathbf{0}, & \text{on } \partial\Omega/\Gamma_{\text{sten}} \\ \sigma(\mathbf{d})\mathbf{n} = & -\mathbf{f_n}, \text{ on } \Gamma_{\text{sten}}, \end{cases} \tag{1}$$

where $\mathbf{d}$ is the displacement vector, $\sigma(\mathbf{d})$ plays the role of the second Piola-Kirchhoff stress tensor and $\mathbf{f_n}$ is a constant normal force applied on a portion of the vein surface (see *e.g.*[4]).

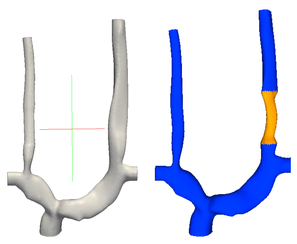

Left: Original geometry. Right: stenosis modeling via artificial reduction of CSA.

Computational fluid dynamics. Considering the blood as an incompressible Newtonian fluid, the velocity field $\mathbf{u}$ and pressure field p in three dimensions are described by the incompressible Navier-Stokes equations (2)

$$\begin{cases} \rho\left(\dfrac{\partial}{\partial t}\mathbf{u} + (\mathbf{u}\cdot\nabla)\,\mathbf{u}\right) = -\nabla p + \nu\Delta\mathbf{u} \\ \nabla\cdot\mathbf{u} = 0. \end{cases} \tag{2}$$

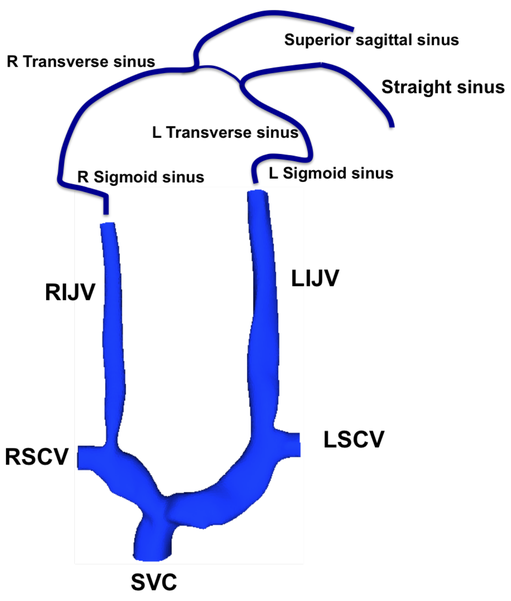

Equations (2) are used to describe the blood flow within the IJVs, neglecting vessels compliance. The upstream circulation, up to the straight and superior sagittal sinuses, is modeled as a network of one-dimensional (1D) compliant tubes. This reduced model can be derived from the mass and momentum conservation equations, in terms of the cross-sectional area $A(x,t)$, the averaged axial velocity $u(x,t)$ and the average internal pressure $p(x,t)$ over the cross-sections:

$$\begin{cases} \partial_t A + \partial_x\left(uA\right) = 0, \\ \partial_t\left(uA\right) + \partial_x\left(Au^2\right) + \dfrac{A}{\rho}\partial_x p = -f, \end{cases} \tag{3}$$

(where f is the friction force due to viscous stresses), plus a closure relation linking $p(x,t)$ to $A(x,t)$ (tube-law).

Multiscale 3D-1D model. The 3D and the 1D models are solved on separate computational domain. For the coupled simulation, the outgoing fluxes from the 1D model are imposed as inlet boundary condition for the velocity at the top of 3D IJVs, while pressures resulting from the 3D solver are imposed at the 1D ends.

Boundary conditions. In all the CFD simulations, patient specific flow rates[7] have been imposed at the inlet boundaries.

Case studies

Starting from a healthy patient geometry, we created 4 stenotic configurations with CSA reduction of 19%, 40%, 66% and 77%, respectively (for the left IJV). For each stenotic case, we considered three different configurations for the confluence of sinuses (disconnected sinuses or existence of weak and strong confluences), modeled as 1D tubes of different radii (Figures a,b,c).

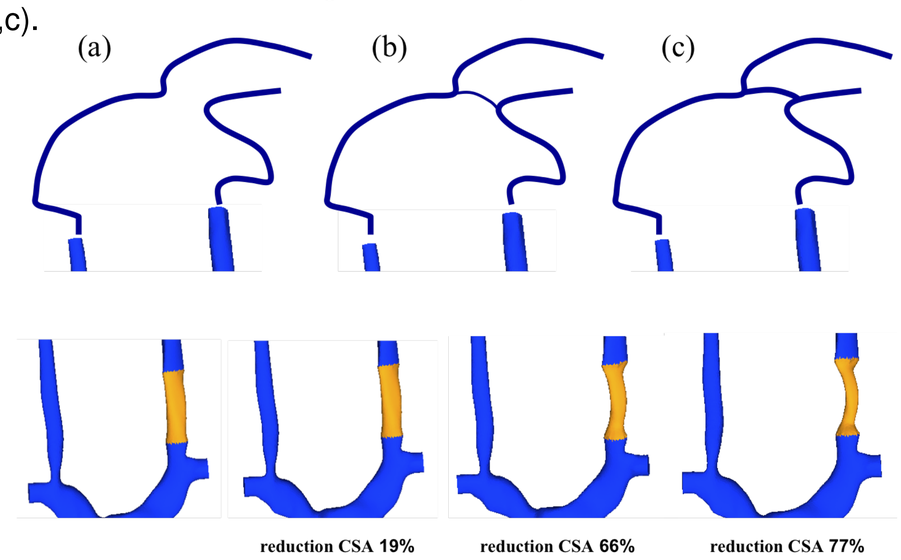

Numerical results

Pressure drop. Figure 1 shows the maximum pressure drop (mmHg) across the IJV throughout a cardiac cycle reduction of CSA (%). We observe an steep increment of pressure drop starting only from an occlusion of about 60 % with respect to the original configuration (CSA reduced from 118 mm^2 to 50mm^2).

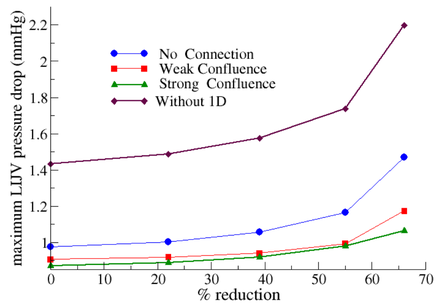

Figure 1

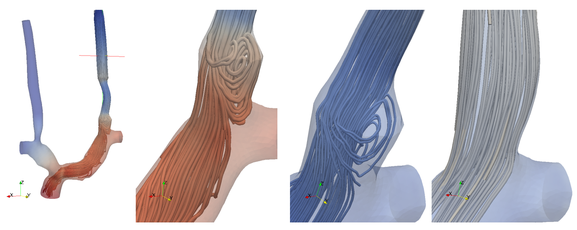

Figure 2

Flow field perturbation. Figure 2 shows the fluid streamlines near the stenosis, for the 3D non compliant simulations (left) and the multiscale 3D-1D model (without sinuses connection) (right). The presence of a stenosis (CSA reduction of 77% in the figure) results in a more disordered flow near the vessel wall and in the appearance of refluxes[6].

Wall-shear stress. We computed the magnitude of the WSS at three selected points: pre-stenotic (top), stenotic (middle) and post-stenotic (bottom) (Figure 3). WSS increases inside the stenotic zone and a decreases in the downstream region. This might be a explained by the formation of recirculation zones near the stenosis, where flow separation occurs (Figure 2). Including a compliant 1D network upstream reduces the impact of the local perturbation.

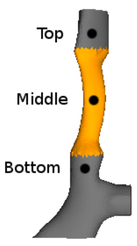

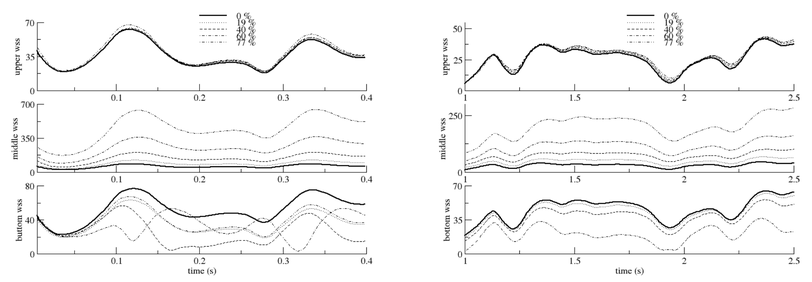

Figure 3

Conclusions

- Through a multiscale computational framework, we evaluated the effect of IJV stenosis of different entities on variable anatomic configurations of collateral paths
- Increment of pressure drop of about 100% (up to 1.5mmHg) for occlusion of 70%
- Small effect for weaker reduction
- Sinuses confluence might eliminate pressure increase acting as baro-regulator
- Flow field is highly perturbed near stenosis (lower wall shear stresses, refluxes)

References

[1] L. Antiga and D. A. Steinman. *IEEE Trans. Med. Imag.*, 23(6):704–713, (2004).
[2] S. A. Berger and L. D. Jou. *Ann. Rev. of Fl. Mech.*, 32:347–382, (2000).
[3] H. Si. Tech. Preprint WIAS, Berlin, 2013.
[4] K. McLeod, A. Caiazzo, M. A. Fernández, T. Mansi, I. E. Vignon-Clementel, M. Sermesant, X. Pennec, Y. Boudjemline, and J.-F. Gerbeau. In *Proc. (STACOM+CESC'10)*, volume 6364 of *LNCS*, pages 95–104, Beijing, 2010. Springer.
[5] T. Papaioannous and C. Stefanadis. *Hellenic J Cardiol*, 46:9–15, (2005).
[6] T. W. Tucker. *Med. Hyp.*, 77:1074–1078, 2011.
[7] W. Feng, D. Utriainen, G. Trifan, S. Elias, S. Sethi, J. Hewett and E.M. Haacke, Neur. Research 34(8): 802–809 (2012)
[8] P. Zamboni, R. Galeotti, E. Menegatti,A. M. Malagoni, G. Tacconi, S. Dall'Ara, I. Bartolomei and F. Salvi, J. Neur. Neurosurgery and Psychiatry. 80:392–399 (2009)

University of Trento *gino.montecinos@ing.unitn.it Via Mesiano 77, 38123 Trento, Italy